[PROC. OF JSCE Structural Eng. / Earthquake Eng. Vol. 2, No. 2 October 1985]

# FATIGUE CRACK GROWTH RATES OF STRUCTURAL STEELS UNDER CONSTANT AND VARIABLE AMPLITUDE BLOCK LOADING

*By Kentaro YAMADA**

Fatigue crack growth rates of structural steels (JIS SS 41, SM 50, SM 58 and HT 80) were measured under constant amplitude and variable amplitude block loadings. The measurement was carried out using Compact-type specimens according to the ASTM E 647-78 T. The fatigue crack growth rates were measured in the range of $\Delta K$ between 10 MPa$\sqrt{m}$ and 35 MPa$\sqrt{m}$. Within the test data, the crack growth rates of all four steels were in good agreement. The variable amplitude block loading was represented by an equivalent stress range computed by the root-mean-cube method, and crack growth rates under variable amplitude block loading were in good agreement with that under constant amplitude loading.

## 1. INTRODUCTION

Fracture mechanics analysis of fatigue crack propagation life using crack growth rates of structural steels and weld metals became more important in understanding fatigue behavior of structural members. This procedure gave engineers keys to evaluate weld deffects, to separate fatigue crack propagation life from fatigue crack initiation life, to consider effect of residual stress on fatigue life, and so on[1)~4)]. The method was extensively used to evaluate the fatigue test results of full scale truss cord members of high strength steels with 800 MPa tensile strength (HT 80 steel). The present fatigue deign specifications and fabrication codes for the Honshu-Shikoku bridges were established based on these fatigue tests and the fracture mechanics analysis[3)].

Numerous fatigue crack growth rates measurements have been reported for various structural steels and weld metals. Although relatively large scatter of data was observed, it has been found that : a) various structural steels showed almost the same fatigue crack growth : b) the fatigue crack growth rates of the weld metal and heat affected zone were similar to that of the base metal : c) residual stress affected the fatigue crack growth rates.

Most structures including highway and railroad bridges are subjected to variable amplitude load fluctuation. The measurement of fatigue crack growth rates have been carried out for various loading patterns ; a) randam variable loads or random variable block loads which simulates the actual loading histogram of the structures ; b) constantly repeated high-low or low-high sequence loads ; c) constant amplitude loads with periodically applied single or multiple overloads[5)-8)]. The test results have been used to study the relation between the constant and variable amplitude block loading, to verify the equivalent

* Member of JSCE, Ph. D., Associate Professor, Department of Civil Engineering, Nagoya University (Furo-cho, Chikusaku, Nagoya)

stress range concepts or Miner's hypothesis, to observe the interaction between the loads, and to observe the growth retardation and delayed retardation behavior due to the crack closure effect. It is of importance for fatigue design of highway and railroad bridges to observe the applicability of the equivalent stress range concepts or the Miner's hypothesis[7)9)].

This report presents the measurement of fatigue crack growth rates for four structural steels under constant and variable amplitude load fluctuation. The results are compared each other to see the effect of material properties and the variable amplitide load patterns on the fatigue crack growth rates.

## 2. TEST PROCEDURE

### (1) Fabrication of Specimens

Fatigue crack growth measurements were carried out basically according to the ASTM E 647-78 T. Four structural steels, Japan Industrial Standards (JIS) SS 41, SM 50, SM 58 Q and HT 80, were used to measure fatigue crack growth rates. Mechanical properties and chemical composition of the steel investigated are shown in Table 1. The Compact-type specimen is shown in Fig. 1. The fatigue crack is to grow perpendicular to the rolling direction of the base metals. Both surfaces of base metals of 10 mm thick was polished by 0.25 mm to obtain 9.5 mm thick specimens. For HT 80 steel, only 20 mm thick plate was available, and about 5 mm thick was polished away from each surface to be used for the specimens.

### (2) Measurement of Fatigue Crack Growth Rates

The loads were applied to the specimens with 5~10 Hz using a closed-loop fatigue testing machine of 250 kN loading capacity. The leading edges of fatigue cracks were monitored periodically on both sides by a pair of travelling microscopes with about 0.01 mm accuracy. The loads were continuously applied to the specimens except for about five minutes when the measurement was carried out.

No overloading was applied to the specimens, even during the pre-cracking phase, to avoid any interaction effect from the previous overloading on the fatigue crack growth rates. Since the loads were constantly applied throughout the measurement, stress intensity factor range, $\Delta K$, gradually increased. All measurements were carried out in ambient condition. Twenty seven (27) specimens were tested under

Table 1 Chemical composition and mechanical properties of steels.

| Steel | Mechanical Properties | | | Chemical Composition (%) | | | | | | | | | |
|---|---|---|---|---|---|---|---|---|---|---|---|---|---|
| | Yield Strength (MPa) | Tensile Strength (MPa) | Elongation $\ell$=200mm (%) | C | Si | Mn | P | S | Cu | Ni | Cr | Mo | V | B |
| SS41 | 353 | 481 | 23 | 0.17 | 0.24 | 0.65 | 0.019 | 0.013 | - | - | - | - | - | - |
| SM50A | 373 | 549 | 23 | 0.18 | 0.22 | 1.30 | 0.015 | 0.011 | - | - | - | - | - | - |
| SM58Q | 579 | 637 | 31 | 0.13 | 0.23 | 1.38 | 0.007 | 0.004 | - | - | - | - | - | - |
| HT80 | 794 | 843 | 36 | 0.11 | 0.26 | 1.01 | 0.010 | 0.002 | 0.17 | 0.82 | 0.48 | 0.32 | 0.003 | 0.001 |

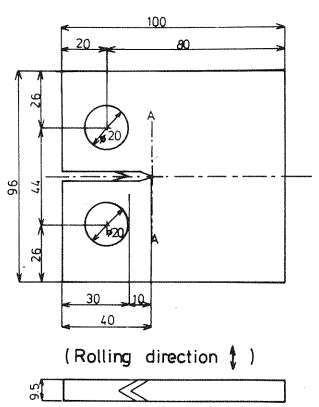


Fig. 1 Compact-type test specimen used to measure fatigue crack growth rates.

Table 2 Test specimens and constant and variable amplitude block loading patterns applied to the specimens.

| Steels | Type of loading | Loading Pattern | No. of Spec. | Range of $\Delta K$ MPa$\sqrt{m}$ |
|---|---|---|---|---|
| SS41 | CA | - | 2 | 10.9 - 32.8 |
| | VA | 2 | 2 | 10.1 - 35.4 |
| SM50A | CA | - | 4 | 11.1 - 58.8 |
| | VA | 1 | 3 | 9.6 - 37.2 |
| | VA | 2 | 3 | 11.4 - 46.6 |
| | VA | 3 | 3 | 9.5 - 38.3 |
| | VA | 4 | 2 | 13.9 - 38.1 |
| SM58Q | CA | - | 2 | 10.5 - 34.5 |
| | VA | 2 | 2 | 9.9 - 35.6 |
| HT80 | CA | - | 2 | 11.3 - 33.5 |
| | VA | 2 | 2 | 10.3 - 35.5 |

constant amplitude (CA) and variable amplitude (VA) load fluctuation, as shown in Table 2.

### (3) Selection of Constant Amplitude Loads

The constant amplitude (CA) loads for fatigue tests were determined such a way that the measurements were carried out normally in the range of $\Delta K$ between 10 and 35 MPa$\sqrt{m}$. According to the previous fatigue crack growth rate measurement, the lower bound of $\Delta K$ of 10 MPa$\sqrt{m}$ gives the crack growth rates of about $5\times10^{-6}$mm/cycle. The ASTM E 647-78 T was assumed to be applicable, although the value was about a half of the lower bound specified by the ASTM procedure.

It has been also reported that the previous measurement showed the rapid decrease of the fatigue crack growth rates at about $\Delta K=10$ MPa$\sqrt{m}$ [4),13)] Normally the loads were gradually decreased to observe the fatigue crack growth rates below this value in order to obtain the threshold level of stress intensity factor range, $\Delta K_{th}$. In the present tests, the loads was kept constant through the test.

Selection of small $\Delta K$ value at the begining of the test may have been yielded unduly delay of the pre-cracking from the chevron notch. However, the $\Delta K$ of this magnitude is often used for the fatigue crack growth analysis. For example, one can assume that an undercut of 0.3 mm deep, torrelance allowed by the specification for the Japanese National Railways, exists at toe of fillet weld. The undercut can then be considered as an edge crack as an unfavorable case. If the applied stress range corresponds to the allowable stress range of $\sigma_{ra}=103$ MPa[11)], the stress intensity factor range for this crack can be computed as follows.

$$K=1.12\cdot F_g\cdot\sigma_r\sqrt{\pi a}$$
$$=1.12\times3\times103\sqrt{\pi\cdot0.0003}$$
$$=10.6\,\mathrm{MPa}\cdot\sqrt{m} \quad \cdots\cdots (1)$$

Where the geometry correction factor for a small crack emanating from the fillet weld toe is assumed as 3.

### (4) Variable Amplitude Block Loading

The variable amplitude (VA) block loading patterns were deduced from a non-dimensionalized stress range histogram, as shown in Fig. 2. The histogram shows an average stress range histogram measured on the short span highway bridges in the United States. More than 100 stress range histograms were first normalized by the maximum stress range and the stress ranges less than 25 percent of the maximum stress range were neglected before taking the average.

Four variable amplitude block loading patterns were determined from the basic stress range histogram. a) Pattern 1 : Stress ranges above 50 percent of the maximum stress range ($\sigma_r/\sigma_{r,max}>0.5$) were retained and devided into five blocks. The number of cycles in this pattern was 1 000 cycles. b) Pattern 2 : Only the

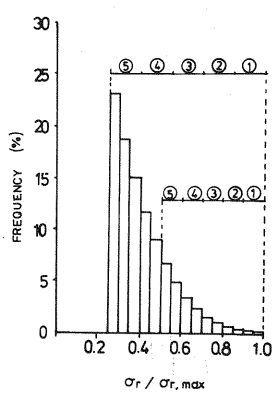


Fig. 2 Basic stress range histogram from which variable amplitude block loading patterns are selected.

Table 3 Variable Amplitude Block Loading Pattern.

| No. | Patterns 1 and 2 Pi/ Pmax | Patterns 1 and 2 ni/N (%) | Patterns 3 and 4 Pi/ Pmax | Patterns 3 and 4 ni/N (%) |
|---|---|---|---|---|
| 1 | 0.95 | 3.4 | 0.925 | 1.2 |
| 2 | 0.85 | 5.2 | 0.775 | 3.3 |
| 3 | 0.75 | 11.9 | 0.625 | 10.9 |
| 4 | 0.65 | 26.7 | 0.475 | 27.6 |
| 5 | 0.55 | 52.8 | 0.325 | 57.0 |
| Prms | 0.638 Pmax | | 0.442 Pmax | |
| Prmc | 0.648 Pmax | | 0.465 Pmax | |

order of the blocks was changed from the Pattern 1. c) Pattern 3 : Stress ranges above 25 percent of the maximum stress range ($\sigma_r/\sigma_{r,\max}>0.25$) were retained and devided into five blocks. This pattern has more number of smaller stress ranges than the Patterns 1 and 2. The number of cycles in this pattern was also 1 000 cycles. d) Pattern 4 : The order and the magnitude of the blocks was the same as the Pattern 3, but this pattern was repeated every 100 cycles.

The number of cycles in each block $n_i$ was listed in Table 3, where $P_i$ is the load range in each block, $\Delta P_{\max}$ is the maximum load range corresponding to the $\sigma_{r,\max}$ in Fig. 2. The equivalent load ranges, $\Delta P_{rms}$ and $\Delta P_{rmc}$, were computed from the following equations.

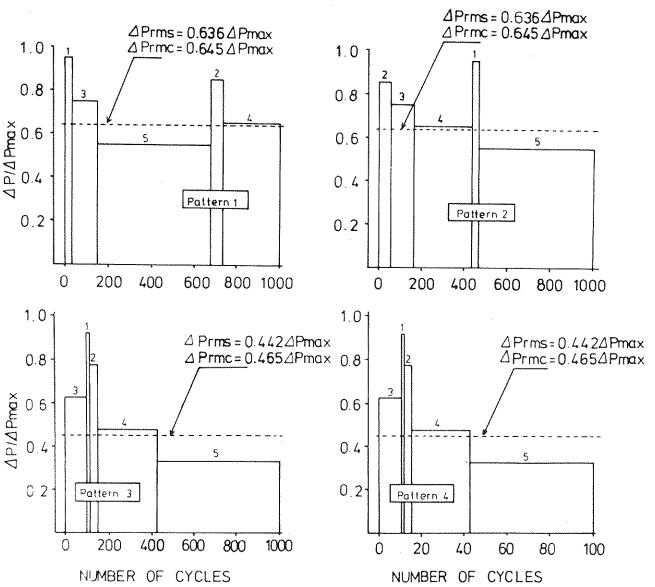


Fig. 3 Types of block loading patterns applied to specimens.

$$\Delta P_{rms}=(\sum n_i \cdot P_i^2/N)^{1/2} \quad (2)$$

$$\Delta P_{rms}=(\sum n_i \cdot P_i^3/N)^{1/3} \quad (3)$$

where $N=\sum n_i$.

The root-mean-square load, $\Delta P_{rms}$, and the root-mean-cube load, $\Delta P_{rmc}$, are equivalent to the Miner's hypothesis when the slopes of $S$-$N$ diagram are two and three, respectively. The diffrence between $\Delta P_{rms}$ and $\Delta P_{rmc}$ values were less than 2 percent for the Petterns 1 and 2, and were about 5 percent for the Petterns 3 and 4. In the experimental design, the block loads were determined in such a way that the root-mean-cube stress intensity factor ranges, $\Delta K_{rmc}$, computed from the $\Delta P_{rmc}$ value were in the range between 10 and 35 MPa$\sqrt{m}$. The data obtained in this range is comparable to that under constant amplitude load fluctuation.

## 3. FATIGUE CRACK GROWTH RATES UNDER CONSTANT AMPLITUDE LOAD

### (1) Fatigue Grack Growth Rates

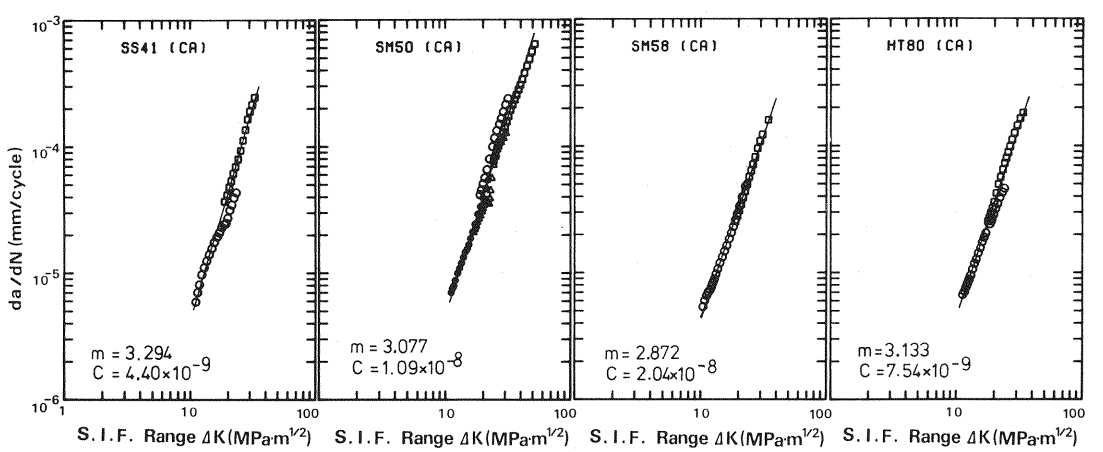


Fig. 4 Constant amplitude fatigue crack growth rates of all four steels.

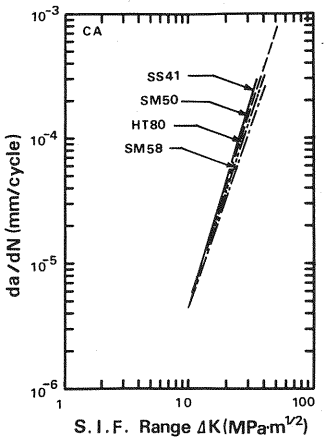


Fig. 5 Summary of constant amplitude fatigue crack growth rates.

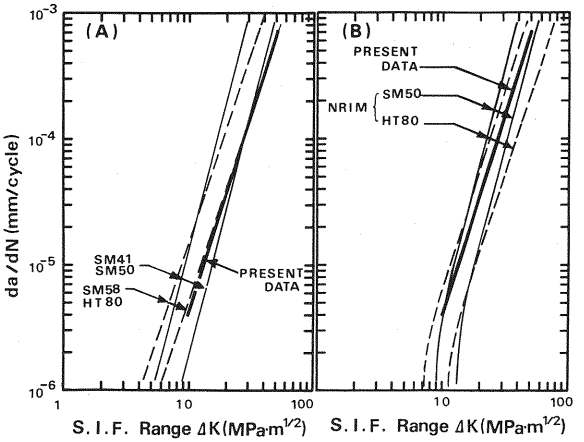


Fig. 6 Comparsion of constant amplitude fatigue crack growth rates with previous investigations.

Four Specimens were used for SM 50 steel for measurement of wider range of $\Delta K$, while two specimens each were used for the other structural steels, as shown in Table 2.

The fatigue crack growth rates of all four steels under constant amplitude loads (CA) are plotted in Fig. 4. Although a little difference in crack growth rates was observed when the data was obtained from more than two specimens, the crack growth rates, $da/dN$, for each steel were linearly correlated with $\Delta K$ on logarithmic scale. Therefore, the crack growth rates can be expressed with the semi-empirical Paris' equation,

$$da/dN = C(\Delta K)^m \quad \cdots\cdots (4)$$

where $C$ and $m$ are material constant determined from the crack growth rates measurement.

The material constant $C$ and $m$ were determined for each steel using the least square method and listed in Fig. 4.

The crack growth rate equations for each steel were replotted in Fig. 5 for comparison. The crack growth rates of all four steels showed almost identical growth rates when stress intensity factor range was small. For example, the crack growth rates were about $4.3\times10^{-6}$ mm/cycle at $\Delta K = 10$ MPa$\sqrt{m}$ for all steels.

A little difference was observed on the crack growth rates of the four steels at the region of higher stress intensity factor range. For example, at $\Delta K = 30$ MPa$\sqrt{m}$, the fatigue crack growth rates were $1.53\times10^{-4}$ mm/cycle for SS 41 steel, $1.40\times10^{-4}$ mm/cycle for SM 50, $1.25\times10^{-4}$ mm/cycle for HT 80, and $1.03\times10^{-4}$mm/cycle for SM 58 Q. The difference is, however, small, if compared with scatter of data in the previous fatigue crack growth rate measurements. Since the fatigue crack propagation life is largely spent when the stress intensitity factor is small, the difference in the fatigue crack growth rates at the higher stress intensity factor range may be negligibly small in the fatigue crack propagation analysis.

Therefore, a single fatigue crack growth rates was computed from the data for all four steels by the least square method.

$$da/dN = 3.11\times10^{-9}(\Delta K)^{3.14} \quad \cdots\cdots (5)$$

where $da/dN$ in mm/cycle and $\Delta K$ in MPa$\sqrt{m}$. Equation 5 was derived from the data of $10 < \Delta K < 58$ MPa$\sqrt{m}$.

### (2) Comparison with Previous Test Data

Numerous fatigue crack growth rate measurements were carried out on the structural steels. Okumura, et al. summarized fatigue crack growth rate equations colleced in Japan and obtained two crack growth rate equations corresponding to structural steels (SM 41 and SM 50 class) and high strength steels (SM 58 and

HT 80 class), as shown in Fig. 6 (A)[12].

The solid lines show the upper and the lower bounds of the crack growth rates equations for SM 41 and SM 50 steels. The material constant $m$ was 4. The dashed lines are for SM 58 and HT 80 steels with the material constant $m=3$. These crack growth rate equations were derived from a variety of crack growth rates equations with various ranges of measurements and various types of specimens, and therefore resulted with large scatter bands. The present test result, expressed by Equation 5, was close to the lower bound for the high strength steels (SM 58 and HT 80), as shown by the solid line in Fig. 5.

The National Research Institute for Metals (NRIM) generated the fatigue crack growth rates of SM 50 B and HT 80 steels[13]. The fatigue crack growth rate equation included the effect of the threshold stress intensity factor range, $\Delta K_{th}$, as follows.

$$da/dN=C(\Delta K^m-\Delta K_{th}^m) \quad (6)$$

It was reported that $m=3.7$ and $\Delta K_{th}=9$ MPa$\sqrt{m}$ for the base metal of SM 50 B steel, and $m=3.0$ and $\Delta K_{th}=6.7$ MPa$\sqrt{m}$ for HT 80 steel. The reported crack growth rate equations are also plotted in Fig. 6 (B). The present test data, plotted by a solid line, was generally within the upper and the lower bounds of both SM 50 B and HT 80 steels. It must be noted that the NRIM data for SM 50 B showed a rapid decrease in crack growth rates when the stress intensity factor range becomes less than about 10 MPa$\sqrt{m}$. The present test data, however, showed no such trend.

It should be also noted that $\Delta K=2.3\sim2.7$ MPa$\sqrt{m}$ was observed for the weld metal of SM 50 B steel. The lower $\Delta K_{th}$ values may attribute to the tensile residual stresses due to welding, which reduces the crack growth retardation effect due to high-low load sequence.

## 4. FATIGUE CRACK GROWTH RATES UNDER VARIABLE AMPLITUDE LOAD

### (1) Fatigue Crack Growth Rates

Fatigue crack growth rates under variable amplitude block loading (VA) of Pattern 2 were measured for all four steels. The test results were plotted in Fig. 7 with a solid lines representing the crack growth rates of the same material under constant amplitude loading. The variable amplitude block loadings were transformed into root-mean-cube load and the equivalent stress intensity factor range $\Delta K_{rmc}$ was computed. Barson et al. used the root-mean-square load $\Delta P_{rms}$ to represent the variable amplitude loadings. The $\Delta P_{rms}$ value was about 1.6 percent less than that of $\Delta P_{rmc}$ for Pattern 2 loading, and it may be negligibly small difference in the practical purpose.

The crack growth rates under variable amplitude block loadings were in good agreement with that under constant amplitude loading, when the variable amplitude block loadings were transformed into the

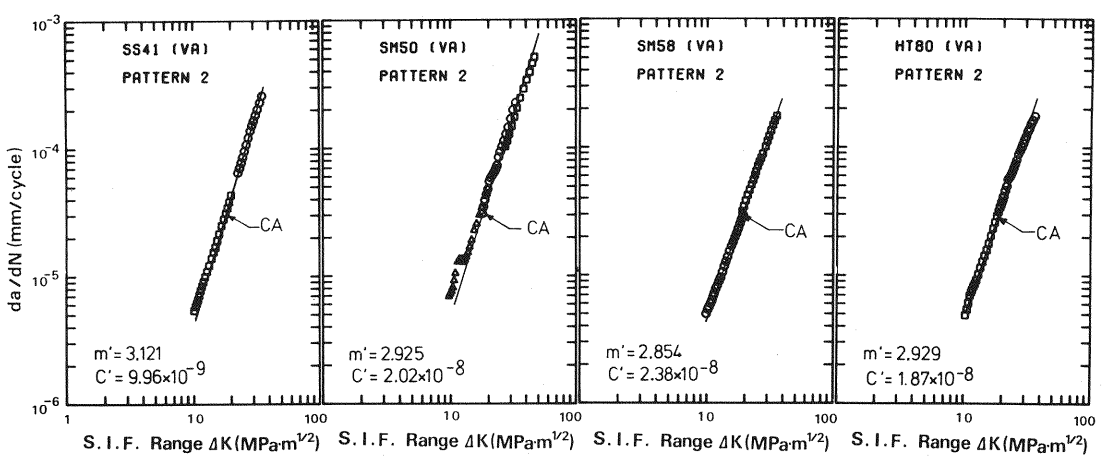


Fig. 7 Variable amplitude fatigue crack growth rates of all four steels.

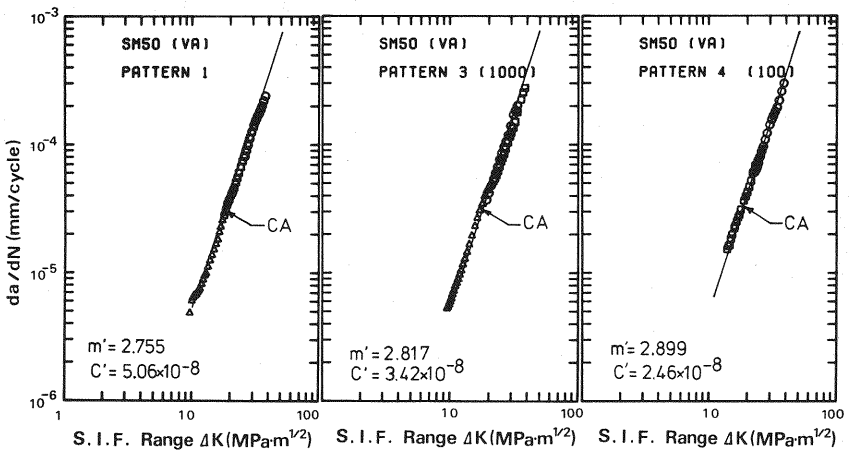


Fig. 8 Effect of variable amplitude block loading patterns on the fatigue crack growth rates of SM 50 steel. (Patterns 1, 3 and 4)

equivalent loads using Eq. 3. The test results for all four steels were in the same tendency.

For SM 50 steel, three other variable amplitude block loading patterns, Patterns 1, 3 and 4, were applied to the specimens for comparison. The test results were also compared with the crack growth rates of SM 50 steel under constant amplitude loading, as shown in Fig. 8. Pattern 1, of which only the order of the block loads differed from pattern 2, gave the same crack growth rates as the constant amplitude loading. The order of the block loads showed little effect on the crack growth rates, when the number of cycles in a pattern was relatively small, for example less than 1 000 cycles[9].

Patterns 3 and 4 includes more cycles with small block loads in the block loading pattern. The crack growth rates under these loading patterns were also in good agreement with that under constant amplitude loadings in the range of measurement. The block loading pattern was repeated every 100 cycles for Pattern 4. No significant effect on the fatigue crack growth rates was observed in this case, which also support the fact that little interaction effect is observed when the number of cycle in a block is relatively small.

Within the range of measurement, it is obvious that a crack growth rate equation can be given in term of the equivalent stress intensity factor range, $\Delta K_{rmc}$, as follows.

$$da/dN = C'(\Delta K_{rmc})^{m'} \quad (7)$$

The regression analysis of all 17 specimens tested under variable amplitude block loadings resulted as $C' = 6.94\times10^{-9}$ and $m' = 2.90$. The crack growth rates corresponding to $\Delta K = \Delta K_{rmc} = 10\ \mathrm{MPa}\sqrt{m}$ for constant and variable amplitude loadings are therefore ;

$da/dN)_{CA} = 4.3\times10^{-6}$ mm/cycle

$da/dN)_{VA} = 5.5\times10^{-6}$ mm/cycle

The crack growth rate under variable amplitude loadings is about 30 percent higher than that under constant amplitude loading. When the crack growth rates corresponding to $30\ \mathrm{MPa}\sqrt{m}$, both give the comparable crack growth rates, as follows.

$da/dN)_{CA} = 1.34\times10^{-4}$ mm/cycle

$da/dN)_{VA} = 1,37\times10^{-4}$ mm/cycle

### (2) Effect of Small Stress Ranges

Each block loading pattern contains ralatively large number of small stress ranges. For example, in Patterns 1 and 2, the smallest block loads of 0.55 of the maximum load range, $\Delta P_{max}$, has 52.8 percent of total number of cycles in the block. Even smaller

Table 4 Variable amplitude block loading patterns and stress intensity factors corresponding to the lowest stress ranges in the pattern.

| Steel | Loading Pattern | a (mm) | $\Delta K_{RMC}$ MPa$\sqrt{m}$ | $\Delta K_{min}$ MPa$\sqrt{m}$ |
|---|---|---|---|---|
| SS41 | 2 | 26.27 | 10.01 | 8.61 |
| SM50 | 1 | 25.26 | 9.61 | 8.20 |
| | 2 | 30.57 | 11.40 | 9.73 |
| | 3 | 24.91 | 9.51 | 6.65 |
| | 4 | 25.26 | 13.89 | 9.70 |
| SM58Q | 2 | 25.69 | 9.91 | 8.45 |
| HT80 | 2 | 26.91 | 10.31 | 8.79 |

block loads of 0.325 of $\Delta P_{max}$ were used for Patterns 3 and 4. The number of cycles of the block loads was 57 percent of the total number of cycles in the block. The strees intensity factor range corresponding to the smallest loads, $\Delta K_{min}$, were between 6.7 and 9.7 MPa$\sqrt{m}$, as shown in Table 4. These values of $\Delta K$ were either less than or close to the threshold values of $\Delta K$, $\Delta K_{th}$, previously measured for the base metals of structural steels. However, the present test data showed no indication of fatigue crack growth reduction at the smaller $\Delta K$ values, even if the large number of small block loadings corresponding less than $\Delta K_{th}$ values were applied.

## 5. CONCLUSION

Fatigue crack growth rates of four structural steels currently used in Japan were measured under constant and variable amplitude block loadings. The structural steels investigated were JIS SS 41, SM 50, SM 58 Q, and HT 80. The test results were compared each other to see the effect of type of steels, variable amplitude block loading patterns, and smaller $\Delta K$ values on the fatigue crack growth rates. The followings summarize the results.

(1) It was confirmed that the fatigue crack growth rates under constant amplitude loadings can be expressed by Paris equation for all structural steels in the range $30<\Delta K<35$ MPa$\sqrt{m}$ (for SM 50 steel the upper limit was about 60 MPa$\sqrt{m}$). The type of the steel had little effect on the fatigue crack growth rates, and a single fatigue crack growth rate equation can be satisfactorily used for all four steels.

(2) Fatigue crack growth rates under variable amplitude block loading can be also expressed by the Paris equation and correlate well with that under constant amplitude loading, when the variable amplitude block loading is transformed into an equivalent stress range using the root-mean-cube method. Measurement was carried out for $10<\Delta K_{rmc}<35$ MPa$\sqrt{m}$.

(3) The variable amplitude block loadings contains relatively large number of block loads of small magnitude, which correspond to small $\Delta K$ values, such as $\Delta K=6.7$ MPa$\sqrt{m}$. Within the measurement, no significant effect of these block loading was observed on the fatigue crack growth rates.

(4) For SM 50 steel, the crack growth rates were measured under the different order of the block loadings and the reduced number of cycles in a block. No significant effect of these variables on the fatigue crack growth rates was observed.

## 6. ACKNOWLEDGEMENT

This study was carried out under the Grant-in Aid for Scientific Research from the Japanese Ministry of Education, in fiscal year of 1983-1984. The author is greatful to Professor Yoichi Kikuchi, Professor Emeritus of Nagoya University, and Dr. Natsume of Yokogawa Bridges for their invaluable suggestion given during the preparation of this paper. The experiment was carried out with the help of Messrs. H. Inagaki, T. Shiozaki, and T. Nomura. Their assistance is greatly acknowledged.

References

1) Committee on Fatigue Strength : Symposium on Fatigue Design based on Fatigue Crack Propagation, FS-481~487-78, Japan Welding Society, 1978 (in Japanese).
2) Yamada, K. et al. : Fracture Mechanics Analysis of Fatigue Crack Emanating From Toe of Fillet Weld, Proc. of JSCE, No. 292, 1979. 12 (in Japanese).
3) Tajima, J. et al. : Welded Structures and Fatigue, Journal of JSCE, Annual 81, Vol. 66-4, 1981 (in Japanese).
4) Ohta, A. et al. : Effect of Residual Stresses on Threshold Level for Fatigue Crack Propagation in Welded Joints of SM 50 B Steel, Journal of Japan Welding Society, Vol. 50, No. 2, 1981 (in Japanese).
5) Barsom, J. M. and Rolfe, S. T. : Fracture and Fatigue Control in Structures, Prectice-Hall, pp. 232~267, 1977.
6) Sasaki, E., Ohata, A. and Kosuge, M. : Fatigue Crack Propagation Rates and Stress Intensity Threshold Level of Several Materials, National Reserch Institute for Metals, 1977.

7) Ito, F. : Fatigue Damage Estimation of Railway Bridges subjected to Service Loadings, Research Report of JNR, No. 796, 1969 (in Japaese).
8) Klippstein, K. H. and Schilling, C. G. : Fatigue Crack Growth under Spectrum Loads, ASTM STP 595, ASTM, pp. 203~216, 1976.
9) Albrecht, P. and Yamada, K. : Simulation of Service Fatigue Loads for Short-Span Highway Bridges, ASTM STP 671, ASTM, pp. 255~277, 1979.
10) ASTM E 647-78 T : Tentative Test Method for Constant-Load Amplitude Fatigue Crack Growth Rates above $10^{-9}$m/cycle.
11) The Japan Society of Civil Engineers : Specifications for Steel Railway Bridges, 1983 (in Japanese).
12) Okumura, T. et al. : Fatigue Crack Growth Rates in Structural Steels, Proceedings of JSCE, No. 322, 1982.
13) Ohata, A. and Sasaki, E. : Fatigue Crack Propagation Properties in Arc welded Butt-Joints of High strength Steels for Welded Structure, NRIM Fatigue Data sheet, Technical Document No. 3, National Research Institute for Metals, 1984.

(Received August 22 1984)